Available online at www.sciencedirect.com

ScienceDirect

Virology 361 (2007) 133–140

VIROLOGY

www.elsevier.com/locate/yviro

Effects of brefeldin A on the localization of *Tobamovirus* movement protein and cell-to-cell movement of the virus

Yuko Tagami, Yuichiro Watanabe *

Department of Life Sciences, Graduate School of Arts and Sciences, The University of Tokyo, Komaba 3-8-1, Meguro, Tokyo 153-8902, Japan

Received 31 August 2006; returned to author for revision 5 October 2006; accepted 8 November 2006
Available online 14 December 2006

Abstract

It has been demonstrated that the subcellular location of *Tobamovirus* movement protein (MP) which was fused with green fluorescent protein (MP:GFP) changed during the infection process. However, the intracellular route through which MP is transported and its biological meaning are still obscure. Treatment with brefeldin A (BFA), which disrupts ER-to-Golgi transport, inhibited the formation of irregularly shaped and filamentous structures of MP. In this condition, MP was still targeted to plasmodesmata in leaf cells. Furthermore, the viral cell-to-cell movement was not inhibited by BFA treatment. These data indicated that the targeting of viral replication complexes (VRCs) to plasmodesmata is mediated by a BFA-insensitive pathway and that the ER-to-Golgi transport pathway is not involved in viral intercellular movement.

Keywords: *Tobamovirus*; Movement protein; Cell-to-cell movement; Brefeldin A; ER-to-Golgi pathway; Plasmodesmata

Introduction

Most plant viruses encode one or more proteins to facilitate spreading from the initially infected cells to adjacent cells, to achieve local and systemic infection in the host. These so-called movement proteins (MPs) enable viruses to exploit plasmodesmata, which provide symplastic continuity and intercellular communication between adjacent cells (Epel, 1994; Heinlein and Epel, 2004). The functions of MP have been well-studied in *Tobacco mosaic virus* (TMV), the type member of the genus, *Tobamovirus* (reviewed in Boevink and Oparka, 2005; Lucas, 2006; Scholthof, 2005; Waigmann et al., 2004). In TMV-infected tobacco plants, as well as in plants transgenically expressing MP, MP accumulates in plasmodesmata and increases their size exclusion limit (SEL) (Waigmann et al., 1994; Wolf et al., 1989). MP also binds single-stranded nucleic acids *in vitro*, forming unfolded and elongated protein-nucleic acid complexes (Citovsky et al., 1990). It is generally accepted that the virus moves from cell to cell in the form of a viral ribonucleoprotein complex (vRNP) (Citovsky et al., 1992; Dorokhov et al., 1984). It is quite possible that MP and vRNP recruit some host components to assist their own translocation through the plasmodesmata.

TMV derivatives that encode MP fused with green fluorescent protein (MP:GFP) have been used to determine in which subcellular compartments MP accumulates. Previous studies demonstrated that MP:GFP fluorescence was localized not only to the plasmodesmata but also to other structures, such as the endoplasmic reticulum (ER) or cytoskeleton, both in protoplasts and leaf cells (Heinlein et al., 1995, 1998; Mas and Beachy, 1999; McLean et al., 1995; Reichel and Beachy, 1998).

Membrane-associated complexes that contain MP, replicase and genomic RNAs are formed, originating from the ER, and have been designated as viral replication complexes (VRCs) (Asurmendi et al., 2004; Mas and Beachy, 1999). Kawakami et al. (2004) demonstrated that the VRC spreads from primary infected cells to secondary infected cells by 20 h post-infection (hpi). But the nature of the motile VRC entity is still obscure. The ER of plants is a dynamic organelle of discrete functional domains (Staehelin, 1997), and the formation of the VRC should be of general interest towards understanding of the plant ER as well as virus movement.

* Corresponding author. Fax: +81 3 5454 6776.
E-mail address: solan@bio.c.u-tokyo.ac.jp (Y. Watanabe).

0042-6822/$ - see front matter © 2006 Elsevier Inc. All rights reserved.
doi:10.1016/j.virol.2006.11.008

Brefeldin A (BFA) is a fungal metabolite known to inhibit the ER-to-Golgi secretory pathway (Nebenfuhr et al., 2002). To investigate the relation between ER-to-Golgi secretory pathway and MP localizations, intracellular locations of MPs of *Grapevine fanleaf virus* (Laporte et al., 2003) and *Cowpea mosaic virus* (Pouwels et al., 2002) were investigated in detail in the presence of BFA. However, these studies were restricted to cultured cells, in which virus cell-to-cell movement ability could not be discussed.

In this study, we used BFA to test whether the ER-related secretory pathway is involved in MP localization and realization of viral cell-to-cell movement in leaves using *Tomato mosaic virus* (ToMV), a member of the *Tobamovirus* family. Our results showed that BFA did not inhibit, at least, the primary establishment of viral trafficking to the adjacent cells, and that MP moves to plasmodesmata via a BFA-insensitive route in infected cells. Using cell fractionation procedures we investigated the intracellular localization of ToMV MP, and tested its association with Golgi bodies and plasma membrane along with the ER, and confirmed that MP is not associated with Golgi bodies. Taking these results together, we could infer that the conventional ER-to-Golgi pathway is not involved in *Tobamovirus* intercellular movement.

Results

The subcellular localization of ToMV MP:GFP

To begin this study of the involvement of the ER-to-Golgi pathway, we first checked the subcellular localization of MP of ToMV in the BY-2 protoplast system, to compare the intracellular localization in detail with previous data from TMV, a virus closely related to ToMV. BY-2 protoplasts were infected with ToMV-MP:GFP, a ToMV expressing MP fused with GFP (Fig. 1) (Kawakami et al., 1999; Kawakami and Watanabe, 1997). MP:GFP fluorescence was examined under a fluorescence microscope until 24 hpi.

We could categorize the fluorescence patterns produced by MP:GFP into five groups (Fig. 2A), based on the fluorescence localization pattern inside the cells. The frequency of protoplasts exhibiting each fluorescence pattern is diagrammed in Fig. 2B. MP:GFP fluorescence was faintly visible at 6 hpi in the ER network (Fig. 2A, ER). At 8 hpi MP:GFP was seen also in peripheral punctate structures (indicated with arrowheads, Fig. 2A) together with scattered ER localization (Fig. 2A, ER+punctate spots). After 8 hpi these punctate spots were visible in most protoplasts with a variety of intracellular complex fluorescence patterns. At 8–14 hpi many irregularly shaped structures were formed inside the cells (Fig. 2A, irregular structures+punctate spots). The structures grew and coalesced to form larger structures, gathering around nuclei and just beneath cell surfaces. At 14–18 hpi MP:GFP seemed to form cytoplasmic bridges between aggregations around the nuclei and below the cell periphery (Fig. 2A, radial filaments+punctate spots). After 20 hpi, MP:GFP was observed in the form of filaments at the cortical region of the cells, in close proximity to the plasma membrane (Fig. 2A, cortical filaments+punctate spots).

Fig. 1. Schematic drawings of viruses. Wild-type ToMV encodes four genes, 126 K and 183 K replication proteins (RdRp), movement protein (MP) and coat protein (CP). ToMV-MP:GFP expresses MP:GFP fusion protein. ToMV-ΔC-GFP expresses GFP under the control of the CP promoter.

From these observations over time, we assumed that two routes of MP intercellular movement were observed together in infected cells. In one route, MP:GFP accumulates at the peripheral punctate spots from early through late stages of infection. In the other route, MP:GFP at first accumulates in the form of irregularly shaped structures around the nuclei, then is transported to the cell periphery via the cytoplasm, and finally forms filamentous structures at the cell cortex during the middle to late stages of infection.

Next we investigated the MP:GFP accumulation patterns in tobacco leaf cells inoculated with ToMV-MP:GFP. Inoculation of leaves with virus expressing the MP:GFP produces fluorescent rings which have newly infected cells at the edges of the rings and cells at the later stages of the infection in the center of the rings (Szecsi et al., 1999). MP:GFP mainly accumulated at the punctate spots (indicated by arrowheads, Fig. 2C) which seemed to be the plasmodesmata at the leading edge of the infection (Fig. 2C, leading edge). In the middle of the fluorescent ring, large irregularly shaped structures were formed (indicated with arrows, Fig. 2C, middle). Filamentous structures were barely visible at the center of the fluorescent rings, which were clearly observed in protoplasts (see above). However, the punctate spots between cells were observed in leaves (Fig. 2C, center). It was previously described that filamentous fluorescence was observed with TMV-MP:GFP in leaf cells (Heinlein et al., 1998). In ToMV, the filamentous fluorescence of MP:GFP in leaves, if any, was much less visible than that in protoplasts. From these observations we consider that the filamentous structures of MP may be unrelated to MP function, i.e., facilitating cell-to-cell movement, as has been previously suggested (Gillespie et al., 2002).

Effect of BFA treatment on ToMV MP:GFP localization in protoplast

Considering the association of MP with the ER, it is possible that ER-to-Golgi membrane trafficking could play a role in MP dynamics and/or functions. To investigate this possibility, we applied BFA and evaluated its effect on subcellular localization and function of MP. BFA is a fungal metabolite known to prevent normal functioning of the ADP-ribosylation factor (ARF) family of small GTPases, followed by Golgi tubulation and fusion with the ER (Nebenfuhr et al., 2002).

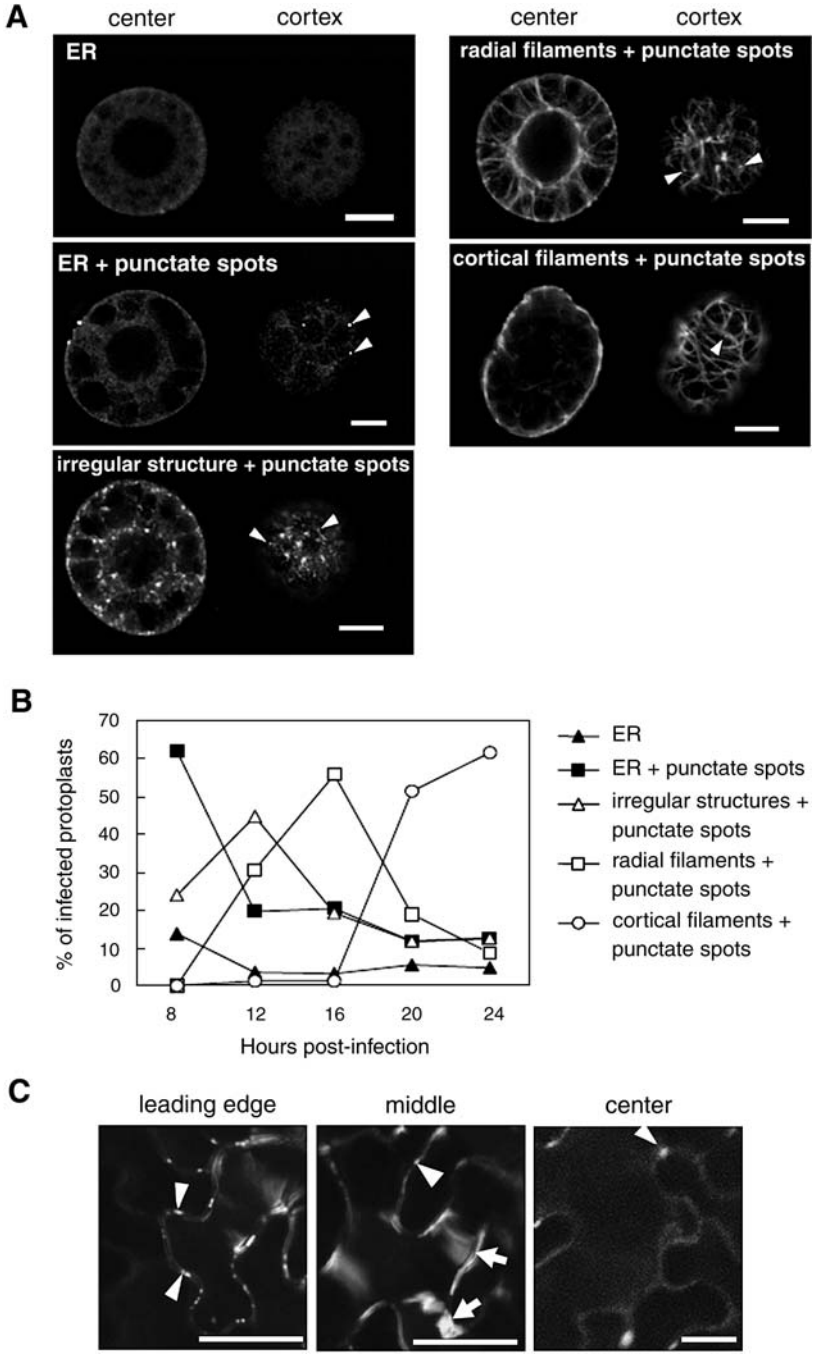

Fig. 2. Changing patterns of MP:GFP fluorescence. (A) Representative images of MP:GFP fluorescent patterns in protoplasts infected with ToMV-MP:GFP. Peripheral punctate spots indicated with arrowheads were observed irrespective of the MP:GFP fluorescence pattern inside the cells. Bars = 10 μm. (ER) MP:GFP fluorescence is observed only at the ER network. (ER + punctate spots) MP:GFP accumulated at the ER and punctate spots at the cell periphery. (Irregular structures + punctate spots) MP:GFP mainly accumulated at irregularly shaped structures together with peripheral punctate spots. (Radial filaments + punctate spots) MP:GFP is observed interlinking the aggregates between the nucleus and cell periphery and at the punctate spots. (Cortical filaments + punctate spots) MP:GFP is accumulated at cortical filamentous structures and punctate spots. (B) Frequency of protoplasts with each MP:GFP fluorescent pattern at indicated time after infection. About 200 cells were counted at each time. (C) MP:GFP fluorescence patterns in leaf cells inoculated with ToMV-MP:GFP at the leading edge, middle, and center of the fluorescent ring. Arrowheads indicate the punctate spots and arrows indicate the irregularly shaped structures. Bars = 100 μm.

To evaluate the effect of BFA on membrane trafficking, a plasmid directing the expression of the Erd2 protein fused to GFP (Erd2:GFP), under control of the cauliflower mosaic virus 35S promoter, was electroporated into protoplasts (Takeuchi et al., 2000). Erd2 is an integral membrane protein localized in the *cis* region of the Golgi apparatus (Lee et al., 1993; Semenza et al., 1990). Therefore, Erd2:GFP fluorescence was used as a marker to observe ER-to-Golgi transport and its inhibition by BFA. In protoplasts expressing Erd2:GFP, fluorescence was observed in many small dots representing Golgi bodies (Fig. 3A, +DMSO). Within 1 h after 10 μg/ml BFA treatment, the "dotty" Golgi pattern changed to an ER network pattern that

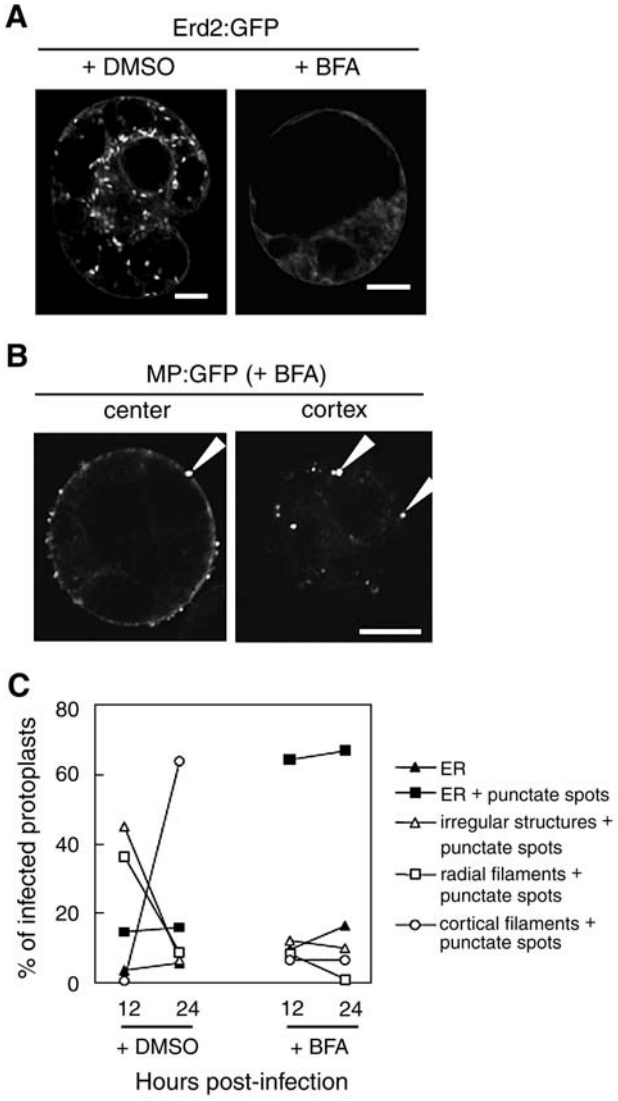

Fig. 3. Effect of brefeldin A on MP:GFP localization in protoplasts. (A) Erd2:GFP (Golgi resident protein) images in protoplasts with or without BFA at 15 h after treatment. Bars = 10 μm. (B) MP:GFP fluorescence in the presence of BFA in protoplasts infected with ToMV-MP:GFP at 12 hpi. Arrowheads indicate the punctate spots at the cell periphery. Bar = 10 μm. (C) Frequency of each MP:GFP fluorescent pattern in protoplasts at indicated time after infection with or without BFA. About 200 cells were counted in each condition.

appeared to spread throughout the cytoplasm (Fig. 3A, +BFA) as has previously been shown (Takeuchi et al., 2000). These data confirmed that our BFA treatment prevented the transport to Golgi bodies from the ER in protoplast system.

To investigate the effect of BFA on MP localization, protoplasts infected with ToMV-MP:GFP were incubated with 10 μg/ml BFA at 1 h after infection. Throughout the infection process, about 60–70% of the cells showed the MP:GFP fluorescence in the ER network and, in addition, clearly at the peripheral punctate spots (Fig. 3B, C). The number of cells showing irregularly shaped structures and filamentous structures was much reduced in the presence of BFA. This observation is not consistent with those observed for TMV-MP:GFP-infected cells treated with BFA (Heinlein et al., 1998). In the protoplasts infected with TMV-MP:GFP, BFA treatment inhibited GFP localization not only in the irregularly shaped structures and filamentous structures but also at the punctate spots (Heinlein et al., 1998). We consider that this may be due to the weak fluorescence of TMV-MP:GFP. When BFA was added to the infected protoplasts at 12 hpi, there was no difference observed in MP:GFP localization relative to the control (data not shown), as has been described previously (Heinlein et al., 1998). Here we reasoned that the MP trafficking to the punctate sites at the cell periphery is not mediated by the ER-to-Golgi secretory pathway, while the formations of irregularly shaped structures and filamentous structures are BFA-sensitive and the Golgi-related secretory pathway may be involved.

Effect of BFA treatment on ToMV MP:GFP localization in leaves

To investigate the effect of BFA on MP:GFP subcellular localization in tobacco leaves, we confirmed that BFA inhibited the ER-to-Golgi pathway in leaves as well as in protoplasts. Tobacco leaves were infiltrated with Agrobacterium carrying Erd2:GFP expressing plasmid and, after 2 days, infiltrated with 10 μg/ml BFA solution. In control leaf cells, Erd2:GFP showed the dotty Golgi pattern as well as in protoplasts (Fig. 4A, +DMSO, 30 min). However, dotty Golgi patterns were disrupted in the presence of BFA in 30 min (Fig. 4A, +BFA, 30 min). This effect persisted until 24 h after BFA treatment (Fig. 4A, +BFA, 24 h). Therefore, we could confirm that BFA prevented ER-to-Golgi secretory pathway in leaf cells until at least 1 day after treatment.

Next we investigated the effect of BFA on MP:GFP subcellular localization in tobacco leaves (Fig. 4B). Leaves inoculated with ToMV-MP:GFP were infiltrated with BFA solution at 2 days post-inoculation (dpi) and MP:GFP was observed 1 day after the BFA treatment. The fluorescence was seen at the spots between cells at the leading edge of the fluorescent ring (Fig. 4B, leading edge) and at the irregularly shaped structures (Fig. 4B, middle) in the middle of the fluorescent ring. These data confirmed that the BFA treatment does not inhibit the MP targeting to punctate spots in leaves as well as in protoplasts. Furthermore, BFA did not have any effect on the irregularly shaped structures once they were established, in the leaves as well as in protoplasts.

Effect of BFA on ToMV cell-to-cell movement

To address the relation between MP localization and viral cell-to-cell transport, we next investigated the ability for cell-to-cell movement of the virus in the presence of BFA. In the leaves inoculated with ToMV-ΔC-GFP (Fig. 1), the sizes of GFP-fluorescence disks reflect the ability of viral cell-to-cell movement (Szecsi et al., 1999). At 2 dpi, tobacco leaves inoculated with ToMV-ΔC-GFP were infiltrated with 10 μg/ml BFA solution or 0.1% DMSO as a control. After 1 day (i.e., 3 dpi) the diameter of GFP fluorescence was measured (Fig. 4C). There was no significant difference in the diameters of the GFP-fluorescence disks between control and BFA-treated

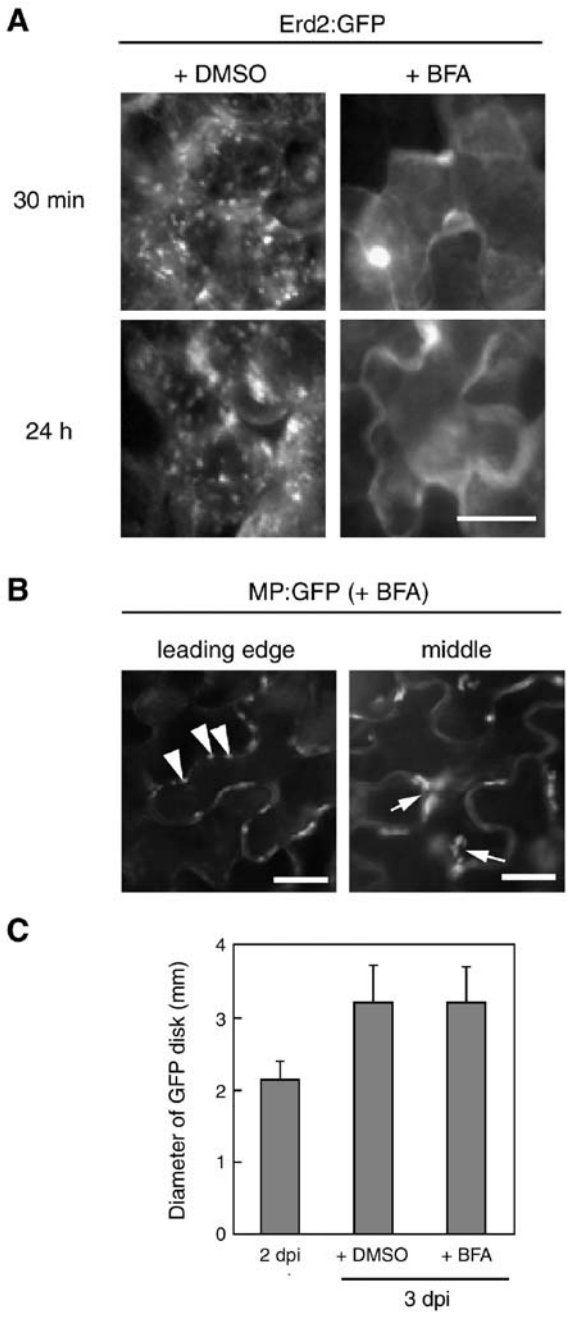

Fig. 4. Effect of brefeldin A on MP:GFP localization in leaves and ToMV cell-to-cell movement. (A) Erd2:GFP images in leaf cells with or without BFA at 30 min and 24 h after treatment. Bar = 50 μm. (B) MP:GFP fluorescence patterns in leaf cells infected with ToMV-MP:GFP 3 days post inoculation and 1 day after BFA treatment. Arrowheads indicate the punctate spots and arrows indicate the irregularly shaped structures. Bars = 50 μm. (C) The average diameters of GFP-disks observed on tobacco leaf inoculated with ToMV-ΔC-GFP before BFA treatment (2 dpi) and 1 day after BFA treatment (3 dpi) (n = 10). DMSO treatment was performed as a control. Bars indicate standard deviations.

leaves, indicating that BFA did not inhibit the cell-to-cell movement of virus. Taken together, these results suggest that the ER-to-Golgi secretory pathway is not involved in MP targeting to plasmodesmata and MP function (viral cell-to-cell transport).

MP is primarily localized to the ER and not trafficked to Golgi bodies

Previous studies using cell fractionation and immunostaining techniques demonstrated that TMV MP was associated with the ER (Heinlein et al., 1998; Mas and Beachy, 1999; Reichel and Beachy, 1998). To investigate the association of ToMV MP with the ER or other organelles, we performed cell fractionation using BY-2 protoplasts infected with ToMV (Fig. 5). Fig. 5A shows the Western blot analysis of MP and marker proteins. Fig. 5B shows the quantification of their distribution patterns shown in Fig. 5A. We used anti-BiP antibody as an ER marker (Hatano et al., 1997), anti-RGP1 antibody as a Golgi complex marker (Dhugga et al., 1997) and anti-PMA2 antibody as a plasma membrane marker (Morsomme et al., 1998).

The main fractions containing MP showed a shift between the absence and presence of Mg^{2+}, MP was alternatively found in fractions 13–15 ($-Mg^{2+}$) and 4–10 ($+Mg^{2+}$). A similar shift appeared in the anti-BiP distributions. While BiP showed very broad distribution patterns, it was mainly detected in fractions 14–17 ($-Mg^{2+}$) and 6–11 ($+Mg^{2+}$). This phenomenon is generally called magnesium-shift and is explained by the fact that ribosomes are bound to the ER in the presence of Mg^{2+} but are released in the absence of Mg^{2+}. Peak fractions of MP also showed the magnesium-shift, while RGP1 and PMA2 did not display this magnesium-shift. Therefore, these data strongly supported the notion that ToMV MP is mainly associated with the ER and not with Golgi bodies. Still, the possibility that MP associated with the plasma membrane could not be eliminated completely because both the minor peak of MP in the absence of Mg^{2+} (fractions 6–10) and the major peak of MP in the presence of Mg^{2+} (fractions 4–10) were overlapped with the peaks of anti-PMA2 (fractions 4–11).

Discussion

In this study we re-examined the time-dependent shift of intracellular localization of MP:GFP fusion protein using ToMV, a different *Tobamovirus* from the well-studied TMV, and its relation to MP function in viral cell-to-cell movement, by focusing on the ER-to-Golgi vesicle transport pathway.

In protoplasts infected with ToMV-MP:GFP, MP:GFP first appeared (at 6–8 hpi) in peripheral punctate structures and persisted in this location throughout infection. At ~14 hpi, MP:GFP also began to accumulate in irregularly shaped structures possibly derived from the ER, as suggested by previous studies with TMV (Heinlein et al., 1998; Mas and Beachy, 1999; Reichel and Beachy, 1998). These irregularly shaped structures were designated as VRCs (viral relplication complexes) which contain MPs, viral replicases and genomic RNAs, and move in the infected cell of an intact plant (Kawakami et al., 2004; Liu et al., 2005). These VRCs grew in size and then disappeared. MP:GFP was redistributed to cortical filamentous structures as well as the peripheral punctate sites that could be seen from the early stages.

BFA, a well-established drug causing inhibition of ER-to-Golgi vesicle transport, altered the MP:GFP temporal shift

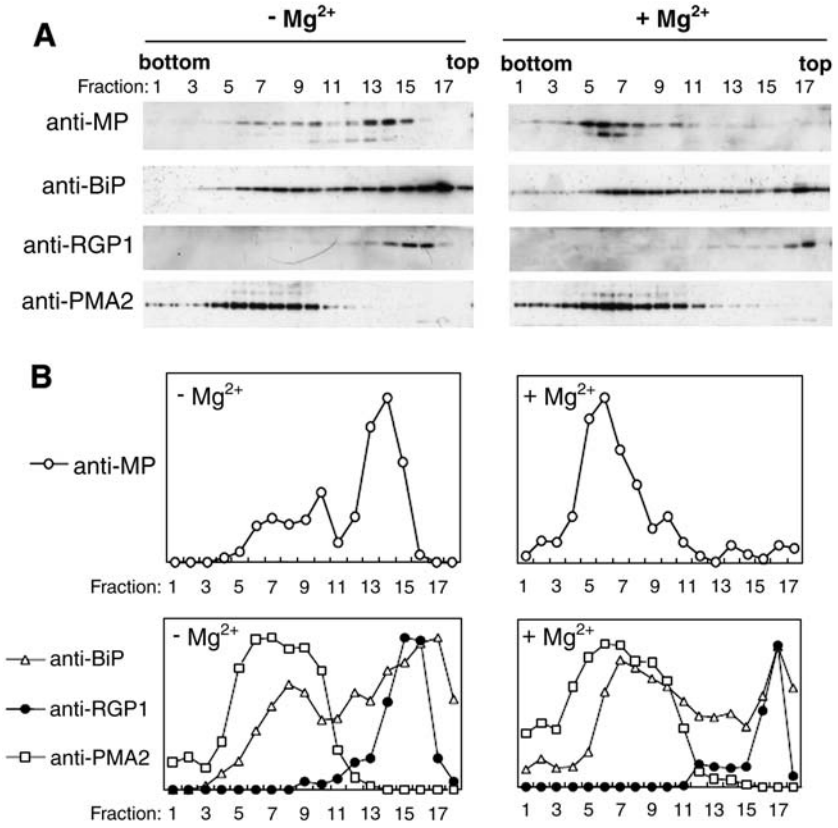

Fig. 5. MP association with ER. (A) Immunoblot analyses of sucrose density gradient fractionation using protoplasts infected with ToMV at 12 hpi. Anti-BiP, RGP1 and PMA2 antibodies are used as ER, Golgi and plasma membrane markers, respectively. The shift in MP location with magnesium treatment is most like the shift observed for anti-BiP fractions, indicating ER association for the MP. (B) Quantified distribution curves of Western blot analyses of (A).

pattern (Fig. 3B, C). In the presence of BFA, MP:GFP was localized only in the ER network and punctate structures at the cell periphery throughout the infection process, but not in the irregularly shaped structures or filamentous structures as was seen in the absence of BFA. These results led us to speculate that two pathways exist for MP subcellular localization, as shown in Fig. 6; (1) MP is transported to plasmodesmata via a BFA-insensitive (Golgi-independent) pathway from the early to late stages of infection. (2) MP forms larger VRCs derived from the ER and is then redistributed to cortical filamentous structures from the middle to the late stages of infection. Because this shift was not observed in the presence of BFA, the modification of Golgi production may affect this process.

The effect of inhibition of ER-to-Golgi transport on ToMV cell-to-cell movement was investigated by using BFA (Fig. 4C). Inhibition of the ER-to-Golgi secretory pathway did not have an effect on cell-to-cell movement of the virus. Considering the effect of BFA on MP localization and the absence of filamentous fluorescence in leaf cells infected with ToMV-MP:GFP (Fig. 2C, center), we reasoned that the formation of large VRCs and targeting of MP to filamentous structures are not required for cell-to-cell movement of virus.

Taking these results together, the mechanism of viral intercellular transport is summarized in Fig. 6. VRCs, derived from the ER membrane, move to plasmodesmata from early to late stages of infection by trafficking possibly along actin filaments (Kawakami et al., 2004; Liu et al., 2005; Szecsi et al., 1999). Plasmodesmata are modified by MP and VMCs (virus movement complexes) to establish propagation to the adjacent cell (Kawakami et al., 2004). This pathway is probably mediated only by the ER membrane because it was not affected

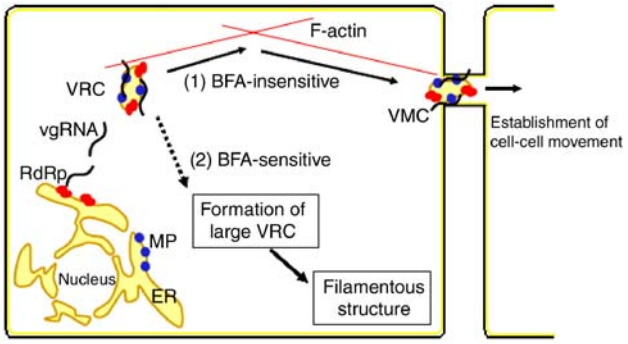

Fig. 6. A model for intracellular dynamics of the ToMV MP and its relationship with virus cell-to-cell movement. In the initially infected cell, viral RdRp is translated and it produces the viral genomic RNA (vgRNA). RdRp, MP and vgRNA accumulate at the ER and form viral replication complexes (VRCs) (Kawakami et al., 2004). VRCs move to plasmodesmata along with actin filaments (Kawakami et al., 2004; Liu et al., 2005) and move to the adjacent cell as a form of virus movement complex (VMC), which is a BFA-insensitive pathway. MPs modify plasmodesmata and facilitate vgRNA transport to adjacent cells. At the same time, VRCs accumulate around the nucleus, move to the cell cortex and form filamentous structures. This is a BFA-sensitive pathway and is not involved in viral cell-to-cell movement. The source of the large VRCs is not clear (indicated with dotted line).

by BFA. On the other hand, VRCs aggregate during the middle stage of infection and move to the cell periphery where they form filamentous structures at the later stages of infection. This activity is possibly mediated by the ER-Golgi pathway because it is inhibited by BFA. It was reported in a study using mutated TMV that large VRCs were not necessary for virus movement (Liu et al., 2005). It was also reported that treatment with proteasome inhibitors prevented the targeting of MP to filamentous structures, indicating that the filamentous arrangement of MP might be involved in viral protein degradation in host cells (Gillespie et al., 2002). Our findings firmly support these previous suggestions.

There are several cases where the endomembrane traffic system of the host is utilized in dissemination of viruses. *Tomato bushy stunt virus* replication protein p33 is localized in novel cytosolic vesicles originating from peroxisomes. Later in infection, it is relocalized to the peroxisomal endoplasmic reticulum (McCartney et al., 2005). It was also reported that the endocytic recycling pathway is involved in the intracellular movement of *Potato mop-top virus* TGB2 and TGB3 (Haupt et al., 2005). Each virus may induce unique intracellular rearrangement strategies for their multiplication and cell-to-cell transport.

Materials and methods

Plant materials

Nicotiana benthamiana plants were grown from seeds and maintained at 22 °C in a growth chamber with a photoperiod of 17 h and a mean photon flux density of 80 μmol m^{-2} s^{-1}. Six- to eight-week-old plants were used for virus inoculation and transient expression.

Viruses

The plasmids pTLQG3 and pTLΔCG3 were used as templates for production of ToMV-MP:GFP and ToMV-ΔC-GFP infectious RNA, respectively (Kawakami and Watanabe, 1997). Schematic representations of viruses are shown in Fig. 1.

Inoculation of virus

Protoplasts were prepared from tobacco BY-2 suspension culture cells and inoculated with infectious transcripts derived from *in vitro* reactions by electroporation, essentially as previously described (Watanabe et al., 1987). Cells (5×10^5) were electroporated with infectious transcripts. After inoculation, 1×10^5 cells were cultured in each 35-mm Petri dish, in the dark at 28 °C. For the inoculation of plants, leaves were dusted with carborundum and gently rubbed with infectious transcripts using brushes.

Transient expression of Erd2:GFP

To confirm the effect of BFA, we used locations of GFP fused with Erd2 (Golgi resident protein) as a marker. For protoplasts, 10 μg of pMT121-AtERD2-GFP (Takeuchi et al., 2000) was used for electroporation as described in "Inoculation of virus". For leaves, leaves of *N. benthamiana* were infiltrated with Agrobacterium carrying pBI121-AtERD2-GFP. Both plasmids were kindly gifted from Dr. Akihiko Nakano (RIKEN).

Treatment with inhibitor

A stock of brefeldin A (BFA, Sigma) was made at 10 mg/ml in DMSO and diluted to 10 μg/ml for use in experiments. Protoplasts were treated with BFA by adding the stock solution into the medium 1 h after infection. Plant leaves were infiltrated into the abaxial side (underside) with BFA solution 2 days after inoculation. In each experiment, treatment with 0.1% DMSO was used as a control.

Microscopic analysis

GFP fluorescence images were observed by fluorescence microscopy using an Olympus IX70-inverted system microscope equipped with an IX-FLA inverted reflected light fluorescence observation attachment and the U-MWIB/GFP filter cube (BP 460–490, DM 505, BA 510IF, Olympus). Images of protoplasts were acquired by using a confocal laser scanning microscope system (LSM 510, Zeiss). Images of leaf cells were acquired using the microscope system, IX-70 and IX-FLA (Olympus) and the software SimplePCI (Compix Inc.). To estimate the frequency of each MP:GFP distribution pattern, about 200 infected protoplasts were counted for each condition. For measuring the diameters of GFP disks, 10 disks were imaged.

Cell fractionation and immunoblot analysis

Protoplasts (1×10^6) infected with ToMV were collected at 12 hpi. Lysis buffer (400 μl; 150 mM Tris–HCl pH 7.5, 10 mM KCl, 1 mM EDTA, 13.5% sucrose, 0.5 mM PMSF, 0.5 μg/ml leupeptin, 0.5 μg/ml pepstatin, with/without 3 mM $MgCl_2$) was added and cells were lysed using a syringe (27 G). Cell lysate was centrifuged at 500×*g* for 5 min. The supernatant was placed onto the sucrose density gradient (100 mM Tris–HCl pH 7.5, 10 mM KCl, 1 mM EDTA, with/without 3 mM $MgCl_2$, 21–55% sucrose) and centrifuged at 100,000×*g* for 14 h (CP70MX, Hitachi). Samples were divided into 18 fractions according to the sucrose density and used for immunoblot analysis.

For immunoblotting, proteins were separated by SDS-PAGE and were blotted onto PVDF membranes (Millipore). As primary antibodies, anti-MP antibody (1:1000; Meshi et al., 1987), anti-BiP antibody (1:1000; Hatano et al., 1997), anti-RGP1 antibody (1:10,000; Dhugga et al., 1997) and anti-PMA2 antibody (1:5000; Morsomme et al., 1998) were used. Anti-rabbit IgG, horseradish peroxidase-linked whole antibody (Amersham Biosciences) was used as the secondary antibody and was detected with ECL plus Western blotting detection reagents (Amersham Biosciences).

Acknowledgments

We thank Drs. Akihiko Nakano, Masaki Takeuchi and Keiko Shoda for Erd2-expressing plasmids, Dr. Ikuko Hara-Nishimura for anti-BiP antibody, Dr. Kanwarpal S. Dhugga for anti-RGP1 antibody, and Dr. Marc Boutry for anti-PMA2 antibody.

References

Asurmendi, S., Berg, R.H., Koo, J.C., Beachy, R.N., 2004. Coat protein regulates formation of replication complexes during tobacco mosaic virus infection. Proc. Natl. Acad. Sci. U.S.A. 101, 1415–1420.

Boevink, P., Oparka, K.J., 2005. Virus–host interactions during movement processes. Plant Physiol. 138, 1815–1821.

Citovsky, V., Knorr, D., Schuster, G., Zambryski, P., 1990. The P30 movement protein of tobacco mosaic virus is a single-strand nucleic acid binding protein. Cell 60, 637–647.

Citovsky, V., Wong, M.L., Shaw, A.L., Prasad, B.V., Zambryski, P., 1992. Visualization and characterization of tobacco mosaic virus movement protein binding to single-stranded nucleic acids. Plant Cell 4, 397–411.

Dhugga, K.S., Tiwari, S.C., Ray, P.M., 1997. A reversibly glycosylated polypeptide (RGP1) possibly involved in plant cell wall synthesis: purification, gene cloning, and trans-Golgi localization. Proc. Natl. Acad. Sci. U.S.A. 94, 7679–7684.

Dorokhov, Y.L., Alexandrova, N.M., Miroshnichenko, N.A., Atabekov, J.G., 1984. The informosome-like virus-specific ribonucleoprotein (vRNP) may be involved in the transport of tobacco mosaic virus infection. Virology 137, 127–134.

Epel, B.L., 1994. Plasmodesmata: composition, structure and trafficking. Plant Mol. Biol. 26, 1343–1356.

Gillespie, T., Boevink, P., Haupt, S., Roberts, A.G., Toth, R., Valentine, T., Chapman, S., Oparka, K.J., 2002. Functional analysis of a DNA-shuffled movement protein reveals that microtubules are dispensable for the cell-to-cell movement of tobacco mosaic virus. Plant Cell 14, 1207–1222.

Hatano, K., Shimada, T., Hiraiwa, N., Nishimura, M., Hara-Nishimura, I., 1997. A rapid increase in the level of binding protein (BiP) is accompanied by synthesis and degradation of storage proteins in pumpkin cotyledons. Plant Cell Physiol. 38, 344–351.

Haupt, S., Cowan, G.H., Ziegler, A., Roberts, A.G., Oparka, K.J., Torrance, L., 2005. Two plant-viral movement proteins traffic in the endocytic recycling pathway. Plant Cell 17, 164–181.

Heinlein, M., Epel, B.L., 2004. Macromolecular transport and signaling through plasmodesmata. Int. Rev. Cytol. 235, 93–164.

Heinlein, M., Epel, B.L., Padgett, H.S., Beachy, R.N., 1995. Interaction of tobamovirus movement proteins with the plant cytoskeleton. Science 270, 1983–1985.

Heinlein, M., Padgett, H.S., Gens, J.S., Pickard, B.G., Casper, S.J., Epel, B.L., Beachy, R.N., 1998. Changing patterns of localization of the tobacco mosaic virus movement protein and replicase to the endoplasmic reticulum and microtubules during infection. Plant Cell 10, 1107–1120.

Kawakami, S., Watanabe, Y., 1997. Use of green fluorescent proteins as a molecular tag of protein movement *in vivo*. Plant Bio/Technol. 14, 127–130.

Kawakami, S., Padgett, H.S., Hosokawa, D., Okada, Y., Beachy, R.N., Watanabe, Y., 1999. Phosphorylation and/or presence of serine 37 in the movement protein of tomato mosaic tobamovirus is essential for intracellular localization and stability *in vivo*. J. Virol. 73, 6831–6840.

Kawakami, S., Watanabe, Y., Beachy, R.N., 2004. Tobacco mosaic virus infection spreads cell to cell as intact replication complexes. Proc. Natl Acad. Sci. U.S.A. 101, 6291–6296.

Laporte, C., Vetter, G., Loudes, A., Robinson, D.G., Hillmer, S., Stussi-Garaud, C., Ritzenthaler, C., 2003. Involvement of the secretory pathway and the cytoskeleton in intracellular targeting and tubule assembly of *Grapevine fanleaf virus* movement protein in tobacco BY-2 Cells. Plant Cell 15, 2058–2075.

Lee, H.I., Gal, S., Newman, T.C., Raikhel, N.V., 1993. The *Arabidopsis* endoplasmic reticulum retention receptor functions in yeast. Proc. Natl. Acad. Sci. U.S.A. 90, 11433–11437.

Liu, J.Z., Blancaflor, E.B., Nelson, R.S., 2005. The tobacco mosaic virus 126-kilodalton protein, a constituent of the virus replication complex, alone or within the complex aligns with and traffics along microfilaments. Plant Physiol. 138, 1853–1865.

Lucas, W.J., 2006. Plant viral movement proteins: agents for cell-to-cell trafficking of viral genomes. Virology 344, 169–184.

Mas, P., Beachy, R.N., 1999. Replication of tobacco mosaic virus on endoplasmic reticulum and role of the cytoskeleton and virus movement protein in intracellular distribution of viral RNA. J. Cell Biol. 147, 945–958.

McCartney, A.W., Greenwood, J.S., Fabian, M.R., White, K.A., Mullen, R.T., 2005. Localization of the *Tomato bushy stunt virus* replication protein p33 reveals a peroxisome-to-endoplasmic reticulum sorting pathway. Plant Cell 17, 3513–3531.

McLean, B.G., Zupan, J., Zambryski, P.C., 1995. Tobacco mosaic virus movement protein associates with the cytoskeleton in tobacco cells. Plant Cell 7, 2101–2114.

Meshi, T., Watanabe, Y., Saito, T., Sugimoto, A., Maeda, T., Okada, Y., 1987. Function of the 30 kd protein of tobacco mosaic virus: involvement in cell-to-cell movement and dispensability for replication. EMBO J. 6, 2557–2563.

Morsomme, P., Dambly, S., Maudoux, O., Boutry, M., 1998. Single point mutations distributed in 10 soluble and membrane regions of the *Nicotiana plumbaginifolia* plasma membrane PMA2 H+-ATPase activate the enzyme and modify the structure of the C-terminal region. J. Biol. Chem. 273, 34837–34842.

Nebenfuhr, A., Ritzenthaler, C., Robinson, D.G., 2002. Brefeldin A: deciphering an enigmatic inhibitor of secretion. Plant Physiol. 130, 1102–1108.

Pouwels, J., Van Der Krogt, G.N., Van Lent, J., Bisseling, T., Wellink, J., 2002. The cytoskeleton and the secretory pathway are not involved in targeting the *Cowpea mosaic virus* movement protein to the cell periphery. Virology 297, 48–56.

Reichel, C., Beachy, R.N., 1998. Tobacco mosaic virus infection induces severe morphological changes of the endoplasmic reticulum. Proc. Natl. Acad. Sci. U.S.A. 95, 11169–11174.

Scholthof, H.B., 2005. Plant virus transport: motions of functional equivalence. Trends Plant Sci. 10, 376–382.

Semenza, J.C., Hardwick, K.G., Dean, N., Pelham, H.R., 1990. ERD2, a yeast gene required for the receptor-mediated retrieval of luminal ER proteins from the secretory pathway. Cell 61, 1349–1357.

Staehelin, L.A., 1997. The plant ER: a dynamic organelle composed of a large number of discrete functional domains. Plant J. 11, 1151–1165.

Szecsi, J., Ding, X.S., Lim, C.O., Bendahmane, M., Cho, M.J., Nelson, R.S., Beachy, R.N., 1999. Development of tobacco mosaic virus infection sites in *Nicotiana benthamiana*. Mol. Plant-Microb. Interact. 12, 143–152.

Takeuchi, M., Ueda, T., Sato, K., Abe, H., Nagata, T., Nakano, A., 2000. A dominant negative mutant of Sar1 GTPase inhibits protein transport from the endoplasmic reticulum to the Golgi apparatus in tobacco and *Arabidopsis* cultured cells. Plant J. 23, 517–525.

Waigmann, E., Lucas, W.J., Citovsky, V., Zambryski, P., 1994. Direct functional assay for tobacco mosaic virus cell-to-cell movement protein and identification of a domain involved in increasing plasmodesmal permeability. Proc. Natl. Acad. Sci. U.S.A. 91, 1433–1437.

Waigmann, E., Ueki, S., Trutnyeva, K., Citovsky, V., 2004. The ins and outs of nondestructive cell-to-cell and systemic movement of plant viruses. Crit. Rev. Plant Sci. 23, 195–250.

Watanabe, Y., Meshi, T., Okada, Y., 1987. Infection of tobacco protoplasts with in vitro transcribed tobacco mosaic virus RNA using an improved electroporation methods. FEBS Lett. 219, 65–69.

Wolf, S., Deom, C.M., Beachy, R.N., Lucas, W.J., 1989. Movement protein of tobacco mosaic virus modifies plasmodesmatal size exclusion limit. Science 246, 377–379.